

Short Note

Evidence for Strong Ground Motion by Waves Refracted from the Conrad Discontinuity

by Xiaobo He and Tae-Kyung Hong

Abstract The Conrad discontinuity, a boundary between the upper and the lower crusts, has long been identified in many continental crusts. The influence of the Conrad discontinuity on seismic hazards, however, has been rarely known. Strong regional phases corresponding to the waves refracted from the Conrad discontinuity are observed in the Korean Peninsula. These phases show strong amplitudes of 2–4 times larger than those of the direct waves. The observation is confirmed by numerical modeling of waveforms. These observations not only support the existence of the Conrad discontinuity in the Korean Peninsula but also suggest the potential of seismic hazards by the Conrad phases. Such strong Conrad-refracted phases are typically recorded in the *Pn* coda portion, which may cause overestimation of *Pn* body-wave magnitudes for regional events.

Introduction

The Conrad discontinuity is a seismically detectable boundary in the continental crust, which has long been identified (e.g., Berry and Fuchs, 1973). The Conrad discontinuity is absent in oceanic crust and sometimes in continental crust with severe tectonic evolutions (e.g., Litak and Brown, 1989). It is known that the Conrad discontinuity is not a physical boundary in which rock composition changes but a seismic impedance-contrast boundary since the Soviet superdeep drilling project during 1970–1994 (Richard, 1989; Pavlenkova, 1993).

Strong Conrad-reflection phases (e.g., *SdS*) and Moho-reflection phases (e.g., *SmS*, *PmP*) have been reported in some regions (e.g., Somerville *et al.*, 1990; Mori and Helmburger, 1996; Chen, 2003; Liu and Tsai, 2009). However, Conrad-refraction phases have rarely been identified. Thus, their importance with respect to seismic hazards has rarely been investigate. Also, the existence of the Conrad discontinuity in the continental regions with severe tectonic evolution history has long been debated (Litak and Brown, 1989; Richard, 1989; Pavlenkova, 1993). The Korean Peninsula is one of the regions. The Korean Peninsula has experienced complex tectonic history including collisions and a rifting, which might have caused dissolution of the Conrad discontinuity.

In this study, we analyze the seismic waveforms of two regional events that occurred in the Korean Peninsula and resolve Conrad phases with the help of numerical modeling of waveforms and travel times. Also, we discuss the implication of Conrad phases on seismic hazards.

Data and Geology

We analyze two regional events in the Korean Peninsula (Fig. 1; Table 1). The event magnitudes are M_L 3.9 and

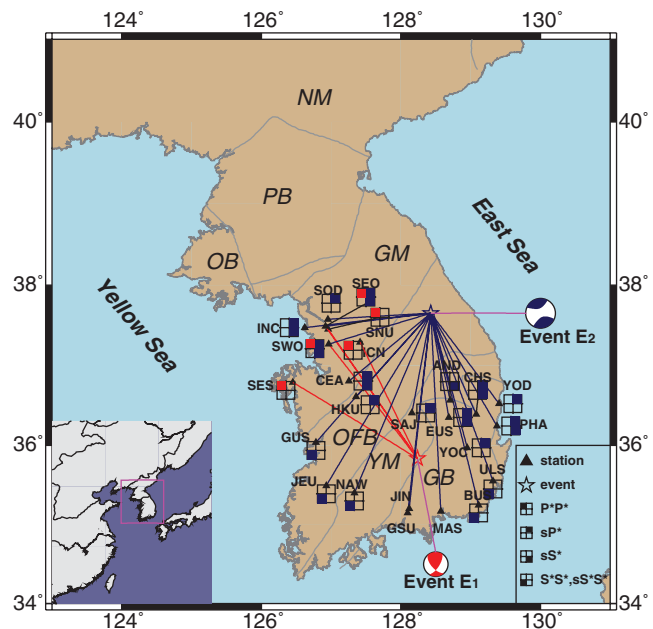


Figure 1. Map of stations (triangles) and earthquakes (stars). The focal mechanisms of the events are presented. The observed Conrad phases (*P*P**, *sP**, *sS**, *S*S**, and *sS*S**) are indicated at every station. Major geological structures are denoted: NM, Nangnim massif; GM, Gyeongsngag massif; YM, Yeongnam massif; PB, Pyeongnam basin; OB, Ongin basin; GB, Gyeongsang basin; and OFB, Okcheon fold belt.

Table 1
Source Parameters of the Earthquakes Analyzed in This Study (Jo and Baag, 2007; Lee and Baag, 2008)

	Origin Date and Time (yyyy/mm/dd; UTC)	Location	Depth (km)	Magnitude	Number of Stations Used
Event E1	2004/04/26 04:29:25	35.836° N, 128.236° E	8.7	M_L 3.9	5
Event E2	2007/01/20 11:56:53	37.686° N, 128.589° E	12.1	M_w 4.5	21

M_w 4.5. The two events produced strong ground motions around the epicenters. The events were well recorded in the Korean seismic networks, yielding high-quality waveform data. We analyze seismic records at stations with epicentral distances less than 300 km.

The Korean Peninsula is located at the eastern margin of the Eurasian plate and links the North and South China blocks to Japanese Islands. The Korean Peninsula has experienced a series of historic tectonic evolutions including continental collision, rifting, and orogeny, which produced lateral heterogeneities in the lithosphere, such as strong lateral variation of crustal and mantle-lid structures (Chough *et al.*, 2000; Chang and Baag, 2007; Hong *et al.*, 2008; Hong and Kang, 2009; Hong, 2010). The Korean Peninsula is composed of three Precambrian massifs including Nangnim, Gyeonggi, and Yeongnam massifs (Fig. 1). It is known that the unification of the three massif blocks into the current shape was completed during the Jurassic period, and the East Sea (Sea of Japan) was opened by continental rifting during the Oligocene and Miocene periods (Chough *et al.*, 2000).

Analyses and Results

Seismic record sections display clear arrivals of multiple crustal phases from both events. We identify seismic phases observed in the record sections. For comparisons with the observed waveforms, we compute synthetic seismograms based on a propagation-matrix technique (Wang, 1999). Synthetic seismograms are calculated for three simple 1D crustal velocity models (Fig. 2). Model A comprises the crustal structure of IASPEI91 (Kennett *et al.*, 1995) overlying a half-space. Models B and C are constructed to include the upper-crustal structure of IASPEI91 over a half-space. Models B and C have the same upper-crustal velocity structure

but have different velocities in half-spaces. Model B has a V_p of 6.5 km/sec, while model C has a V_p of 6.0 km/sec. The S -wave velocities of models B and C for half-spaces are assigned as $V_p/1.73$ with an assumption of a Poisson solid. These models allow us to calculate only the crustal phases, including Conrad-discontinuity phases. The Global Centroid Moment Tensor (CMT; see the [Data and Resources](#) section) solution is used for the source mechanism of event E1, and the solution of Lee and Baag (2008) is used for event E2. We conduct a ray tracing, and determine the ray paths of the later phases (Crotwell *et al.*, 1999). The ray paths and reduced travel-time curves of representative crustal phases are presented in Figure 3. Vertical velocity seismograms clearly show multiple crustal-phase arrivals (Figs. 4–6).

For event E1, large-amplitude phases, about 2–4 times stronger than Pg , are observed in the Pg coda (Fig. 4). These phases are identified as the double-refracted Conrad phase P^*P^* , which is confirmed by synthetic calculations of travel times and waveforms (Fig. 4). The strong, later phases are well reproduced from both models A and B (see, central column of Fig. 4). Because the Moho discontinuity exists only in model A, we conclude that these phases are not generated by the Moho but the Conrad discontinuity. We also observe clear differences in arrival times for these phases between models B and C (see, right-hand column of Fig. 4). The observation supports that the large-amplitude phases are not reflected waves but refracted waves from the Conrad discontinuity.

We also observe another pronounced phase at stations SWO, SES, and ICN between Pn and P^*P^* in Figure 4. We expect similar travel times between the Conrad-refracted phase P^* and the Moho-reflected phase PmP . Thus, it appears that both P^* and PmP contribute to this phase, which is also seen for event E2 in Figure 5a. A similar feature is observed between Sn and S^*S^* as shown in Figure 6b,

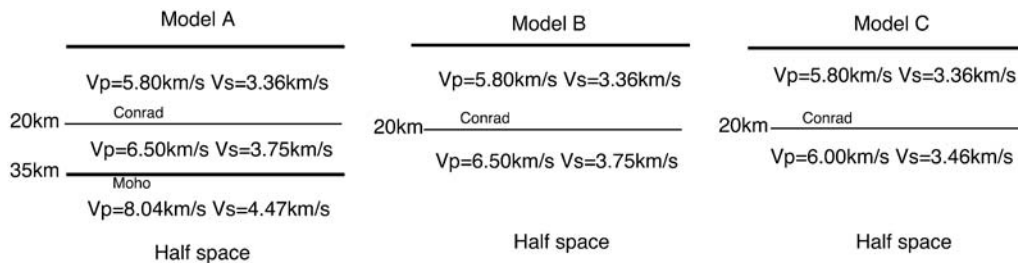


Figure 2. A schematic illustration of three crustal models incorporated for calculation of synthetic seismograms. Model A comprises the crustal structure of IASPEI91 (Kennett *et al.*, 1995) overlying a half-space. Models B and C are constructed to include the upper-crustal structure of IASPEI91 over a half-space. The upper-crustal structures are the same between models B and C, but model C has lower velocities in the half-space than model B. The S -wave velocity in the half-space of model C is assigned as $V_p/1.73$ with the assumption of a Poisson solid. Models B and C produce only the upper-crustal phases along with Conrad-discontinuity phases.

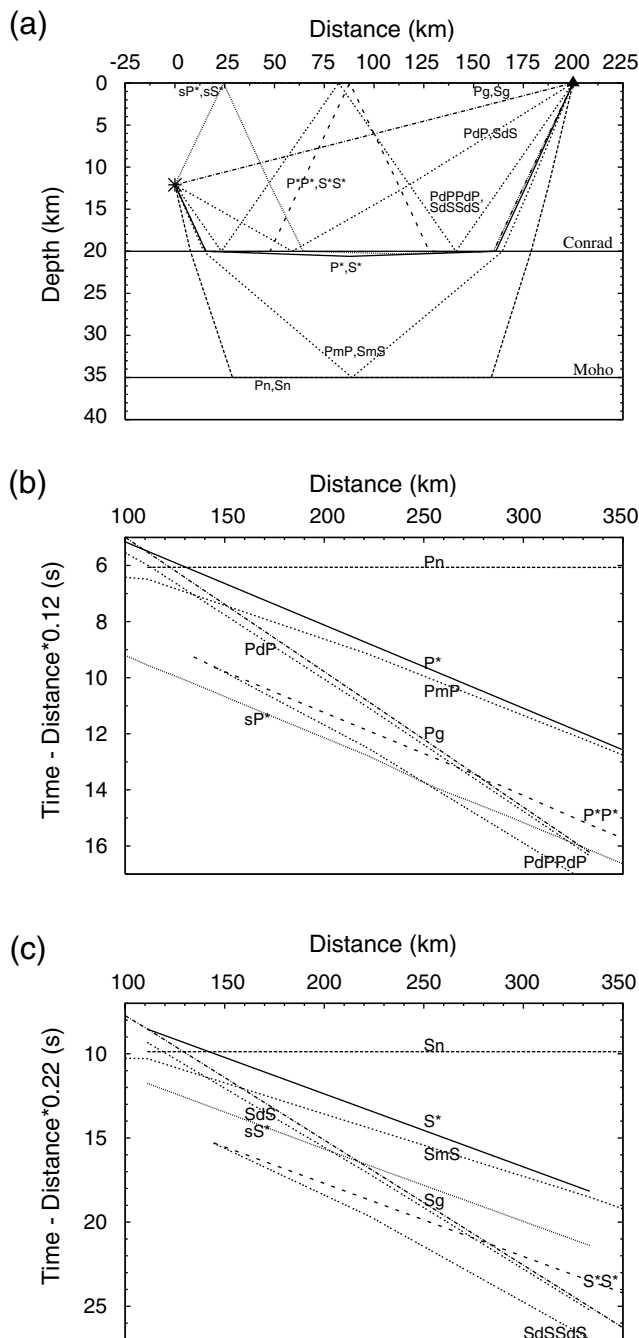


Figure 3. (a) A schematic illustration of ray paths of crustal and Moho-refraction and Moho-reflection phases, and corresponding travel-time curves of (b) P and (c) S phases for an event with a focal depth of 12.1 km. The phase names are annotated. The phases include PdP and SdS (Conrad-reflection phases), $PdPPdP$ and $SdSSdS$ (double Conrad-reflection phases), P^* and S^* (Conrad-refraction phases), sP^* and sS^* (Conrad-refraction depth phases), P^*P^* and S^*S^* (double Conrad-refraction phases), PmP and SmS (Moho-reflection phases), Pn and Sn (Moho-refraction phases), and Pg and Sg (direct waves).

where the phase is comprised of both the S Conrad-refraction phase S^* and the S Moho-reflection phase SmS .

In Figure 5a, we find that P^*P^* has a similar arrival time with Pg . We rarely find any difference in synthetic wave-

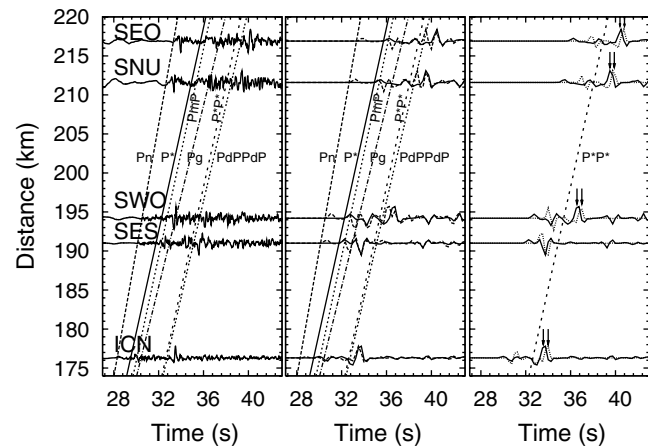


Figure 4. Comparisons of observed seismograms and corresponding synthetic seismograms. The left-hand column displays the observed vertical seismograms of event E1. The corresponding synthetic seismograms in the central and right-hand columns are based on models A and B, and models B and C, respectively (see, Fig. 2). Synthetic seismograms calculated for models A, B, and C are denoted by solid, dashed, and dotted lines, respectively. Every record section is normalized by its peak amplitude. Seismograms and station codes are plotted with respect to their epicentral distances. Theoretical travel-time curves based on IASPEI91 are superimposed. Models A and B produce similar waveforms in the Pg coda portions in the central column, suggesting that the later large-amplitude phases are not associated with a Moho. Waveforms with different arrival times are marked with arrows in the right-hand column, suggesting that the later phases are not reflected waves but refracted waves. Another pronounced phase is observed between Pn and P^*P^* at stations SWO, SES, and ICN.

forms and travel times between models B and C. This observation suggests that the strong phase may be contributed more by Pg than by P^*P^* . This feature may be caused due to the source radiation pattern; as shown in Figure 1, stations GSU, MAS, and JIN have similar azimuths to event E2. This observation suggests that the Conrad-refracted phases are strongly dependent on the source radiation pattern.

In addition, the Conrad-refracted S -depth phases, sP^* and sS^* , are identified in Figures 5b and 6a, respectively. Most wave trains display a strong sP^* of which amplitudes are comparable to those of Pg , while sS^* shows 2–3 times larger amplitudes than Sg . We also observe strong double-refracted S Conrad phases, S^*S^* and sS^*S^* , which have amplitudes that are similar to each other (Fig. 6b). All the observations are confirmed by synthetic waveforms. The synthetic traces display high similarity in waveforms between models A and B. However, we find that the later phases display arrival-time differences between models B and C (arrows in Figs. 5b and 6). The observations indicate that the later, large-amplitude phases are not Conrad-reflected or Moho-reflected phases but Conrad-refracted phases.

The large amplitudes of the Conrad phases allow us to identify these phases easily in the near-regional seismograms. The observed Conrad phases are well reproduced in synthetic seismograms, although slight differences in the arrival times are found between the field and synthetic

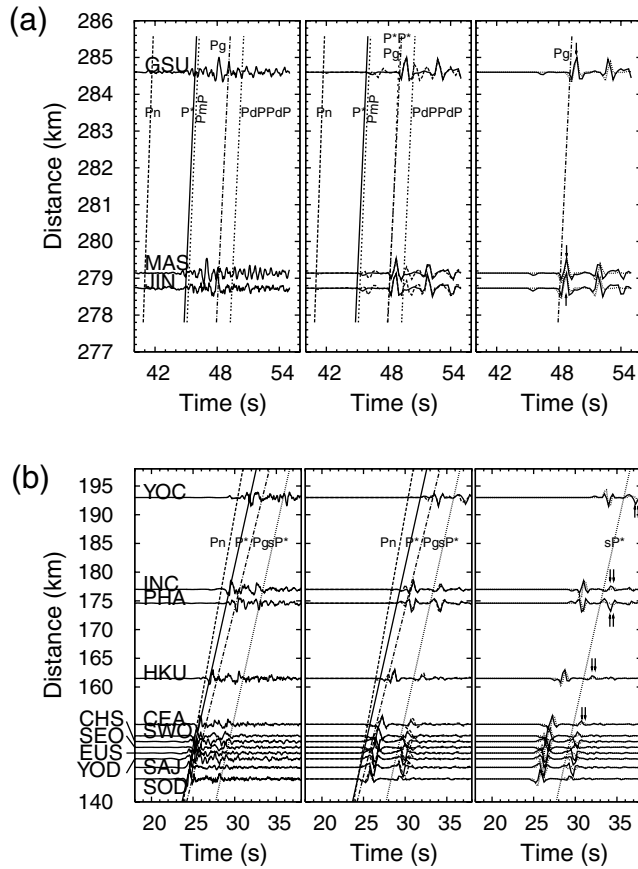


Figure 5. Comparisons of observed vertical seismograms of P -wave trains (left-hand columns) and corresponding synthetic seismograms based on models A and B (central columns) and based on models B and C (right-hand columns) for event E2: (a) seismograms for distances between 277 and 285 km and (b) between 140 and 195 km. Synthetic traces calculated for models A, B, and C are denoted by solid, dashed, and dotted lines, respectively. Every record section is normalized by its peak amplitude. Seismograms and station codes are plotted with respect to their epicentral distances. Theoretical travel-time curves based on IASPEI91 are superimposed. The peaks of the later phases reproduced by models B and C are marked with arrows. There are no differences in travel times of these phases between models B and C in (a), while obvious differences are observed in (b).

seismograms (Figs. 4–6). The arrival-time misfits may be caused due to incorporation of a 1D crustal model that does not reflect the local heterogeneities in the crust sufficiently.

Discussion and Conclusions

Strong later phases are consistently observed at dozens of stations deployed over the southern Korean Peninsula. We identified the phases with the help of synthetic seismograms based on three different crustal models overlying half-spaces (Fig. 2). The strong later phases were reproduced from all the models. The observation enables us to rule out the possibility of association of these phases with the Moho. Arrival-time differences of the later phases are clearly observed between models B and C (Figs. 4, 5b, and 6). The observation suggests

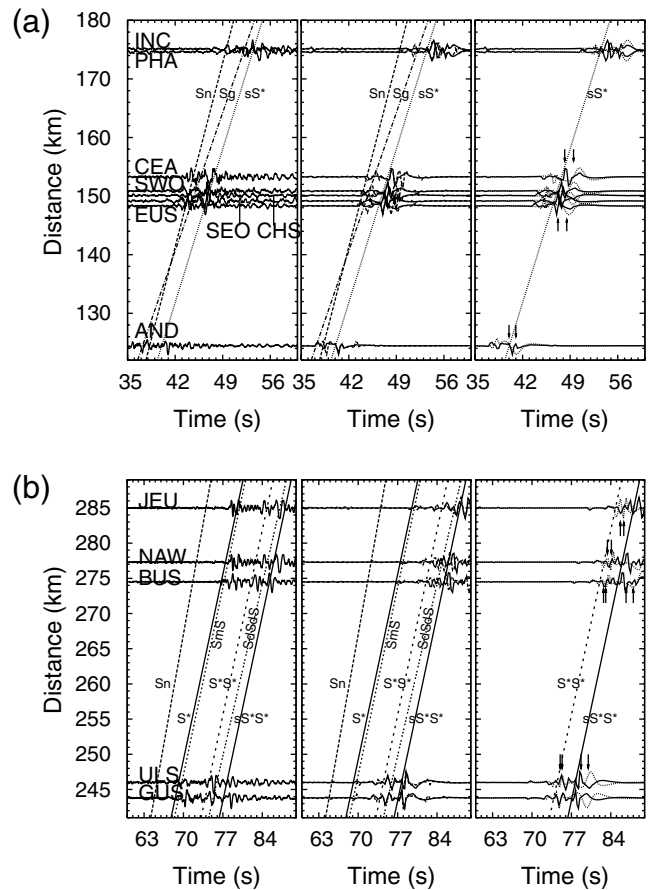


Figure 6. Comparisons of observed vertical seismograms of S -wave trains (left-hand columns) and corresponding synthetic seismograms based on models A and B (central columns) and based on models B and C (right-hand columns) for event E2: (a) seismograms for distances between 122 and 180 km and (b) between 140 and 195 km. Synthetic traces calculated for models A, B, and C are denoted by solid, dashed, and dotted lines, respectively. Every record section is normalized by its peak amplitude. Seismograms and station codes are plotted with respect to their epicentral distances. Theoretical travel-time curves based on IASPEI91 are superimposed. The peaks of the later phases reproduced by models B and C are marked with arrows. Obvious differences in travel times of these phases are observed in both (a) and (b).

that these phases are not reflected waves but refracted waves. Thus, we confirm that the later, large-amplitude phases are Conrad-refracted phases. The identification of such phases suggests that a Conrad discontinuity exists in the Korean Peninsula, a region with complex tectonic evolution history.

We also find that the strong Conrad phases are important for seismic hazards because they can produce strong ground motion at near-regional distances. Models A and B produce similar synthetic waveforms in the traces after the Moho-refraction and crustal direct phases, which suggests that the large-amplitude phases are associated with the upper-crustal structure. Thus, crustal geologic structures are important for the assessment of ground motions by local and near-regional earthquakes.

It is noteworthy that strong Conrad- and Moho-reflected phases (e.g., *ScS*, *SmS*, and *PmP*) are developed from a Conrad and Moho with high impedance contrast (e.g., [Somerville et al., 1990](#); [Mori and Helmberger, 1996](#); [Chen, 2003](#); [Liu and Tsai, 2009](#)). Thus, large-amplitude Conrad- and Moho-reflected phases are observed in limited regions (e.g., [Somerville, et al., 1990](#); [Mori and Helmberger, 1996](#)). However, strong Conrad-refracted phases are well developed from crustal models. The observation suggests that such Conrad-refracted phases can be observed widely over the globe. Thus careful consideration of the influence of the Conrad-refracted phases may be required for evaluation of seismic hazards.

Also, we find that a strong Conrad-refracted phase P^* is often observed in the *Pn* coda portion. Because a *Pn* body-wave magnitude scaling is based on the wave trains including both *Pn* and *Pn* coda, *Pn* magnitude can be overestimated without careful measurement of phase amplitude. In addition, the identified Conrad phases can provide constraints to refine the upper-crustal structure, which is difficult to study with conventional techniques, such as travel-time tomography of direct waves and receiver function analyses.

Data and Resources

Seismic waveform data used in this study were collected from the Web sites of the Korea Meteorological Administration (KMA; www.kma.go.kr, last accessed August 2008) and the Korea Institute of Geoscience and Mineral Resources (KIGAM; quake.kigam.re.kr, last accessed August 2008). The Global Centroid Moment Tensor Project database is available at www.globalcmt.org/CMTsearch.html. Some figures were produced using Generic Mapping Tools (GMT; [Wessel and Smith, 1995](#); gmt.soest.hawaii.edu, last accessed September 2008) and GNPLOT (www.gnplot.info, last accessed September 2008).

Acknowledgments

The authors are grateful to the Korea Meteorological Administration (KMA) and the Korea Institute of Geoscience and Mineral Resources (KIGAM) for providing the seismic waveform data. Much of the seismic waveform analyses were carried out using the Seismic Analysis Code (SAC). All maps of this study were prepared with GMT ([Wessel and Smith, 1995](#)) and GNPLOT (www.gnplot.info). This work was supported by the Korea Meteorological Administration Research and Development Program under Grant Number CATER 2007-5111. X. H. was partly supported by the Yonsei University Postdoctoral Research Fund of 2009.

References

Berry, M. J., and K. Fuchs (1973). Crustal structure of the superior and Grenville provinces of the Northeastern Canadian Shield, *Bull. Seismol. Soc. Am.* **63**, 1393–1432.

- Chang, S.-J., and C.-E. Baag (2007). Moho depth and crustal V_p/V_s variation in southern Korea from teleseismic receiver functions: Implication for tectonic affinity between the Korean Peninsula and China, *Bull. Seismol. Soc. Am.* **97**, 1621–1631.
- Chen, K.-C. (2003). Strong ground motion and damage in the Taipei basin from the Moho reflected seismic waves during the March 31, 2002, Hualien, Taiwan earthquake, *Geophys. Res. Lett.* **30**, no. 11, 1515, doi 10.1029/2003GL017193.
- Chough, S. K., S.-T. Kwon, J.-H. Ree, and D.-K. Choi (2000). Tectonic and sedimentary evolution of the Korean peninsula: A review and new view, *Earth Sci. Rev.* **52**, 175–235.
- Crotwell, P. H., T. J. Owens, and J. Ritsema (1999). The TauP toolkit: Flexible seismic travel-time and raypath utilities, *Seism. Res. Lett.* **70**, 154–160.
- Hong, T.-K. (2010). *Lg* attenuation in a region with both continental and oceanic environments, *Bull. Seism. Soc. Am.* **100**, no. 2, 851–858.
- Hong, T.-K., and T.-S. Kang (2009). *Pn* travel-time tomography of the Paleo–continental–collision and rifting zone around Korea and Japan, *Bull. Seismol. Soc. Am.* **99**, 416–421.
- Hong, T.-K., C.-E. Baag, H. Choi, and D.-H. Sheen (2008). Regional seismic observations of the 9 October 2006 underground nuclear explosion in North Korea and the influence of crustal structure on regional phases, *J. Geophys. Res.* **113**, B03305, doi 10.1029/2007JB004950.
- Jo, N., and C.-E. Baag (2007). The 20 January 2007, M_w 4.5, Odaesan, Korea, earthquake, *Geosci. J.* **11**, 51–58.
- Kennett, B. L. N., E. R. Engdahl, and R. Buland (1995). Constraints on seismic velocities in the Earth from travel times, *Geophys. J. Int.* **122**, 108–124.
- Lee, W., and C.-E. Baag (2008). Local crustal structures of southern Korea from joint analysis of waveforms and travel times, *Geosci. J.* **12**, 419–428.
- Litak, B. K., and L. D. Brown (1989). A modern perspective on the Conrad discontinuity, *Eos Trans. Am. Geophys. Union* **70**, 713.
- Liu, K.-S., and Y.-B. Tsai (2009). Large effects of Moho reflections (*SmS*) on peak ground motion in Northwestern Taiwan, *Bull. Seismol. Soc. Am.* **99**, 255–267.
- Mori, J., and D. Helmberger (1996). Large-amplitude Moho reflections (*SmS*) from Landers aftershocks, Southern California, *Bull. Seismol. Soc. Am.* **86**, 1845–1852.
- Pavlenkova, N. I. (1993). The Kola superdeep drillhole and the nature of seismic boundaries, *Terra Nova* **4**, 117–123.
- Richard, A. K. (1989). Deep holes yielding geoscience surprises, *Science* **245**, 468–470.
- Somerville, P. G., J. P. McLaren, C. K. Saikia, and D. V. Helmberger (1990). The 25 November 1988 Saguenay, Quebec, earthquake: Source parameters and the attenuation of strong ground motion, *Bull. Seismol. Soc. Am.* **80**, 1118–1143.
- Wang, R. (1999). A simple orthonormalization method for stable and efficient computation of Green's functions, *Bull. Seismol. Soc. Am.* **89**, 733–741.
- Wessel, P., and W. H. F. Smith (1995). New version of the Generic Mapping Tool released, *Eos Trans. AGU* **76**, 329.

Department of Earth System Sciences
Yonsei University
Shincheon-dong, 134, Seodaemun-gu
Seoul 120-749, South Korea
xiaobo@yonsei.ac.kr
tkhong@yonsei.ac.kr

Manuscript received 1 July 2009